Supporting Information: Structure and Mechanical Properties of Grain Boundaries in Molybdenum Disulfide (MoS_2)

Robert D. Moore,[†] N. Scott Bobbitt,[‡] Ian S. Winter,[‡] John F. Curry,[‡] Lisa Levandosky,[†] Sophia Renaud,[¶] Michael Chandross,[*,‡] and Fadi Abdeljawad[*,†]

†*Department of Materials Science and Engineering, Lehigh University, Bethlehem, PA, 18015 USA*

‡*Material, Physical, and Chemical Sciences Center, Sandia National Laboratories, Albuquerque, NM, 87123 USA*

¶*Department of Bioengineering, Lehigh University, Bethlehem, PA, 18015 USA*

E-mail: mechand@sandia.gov; fadi@lehigh.edu

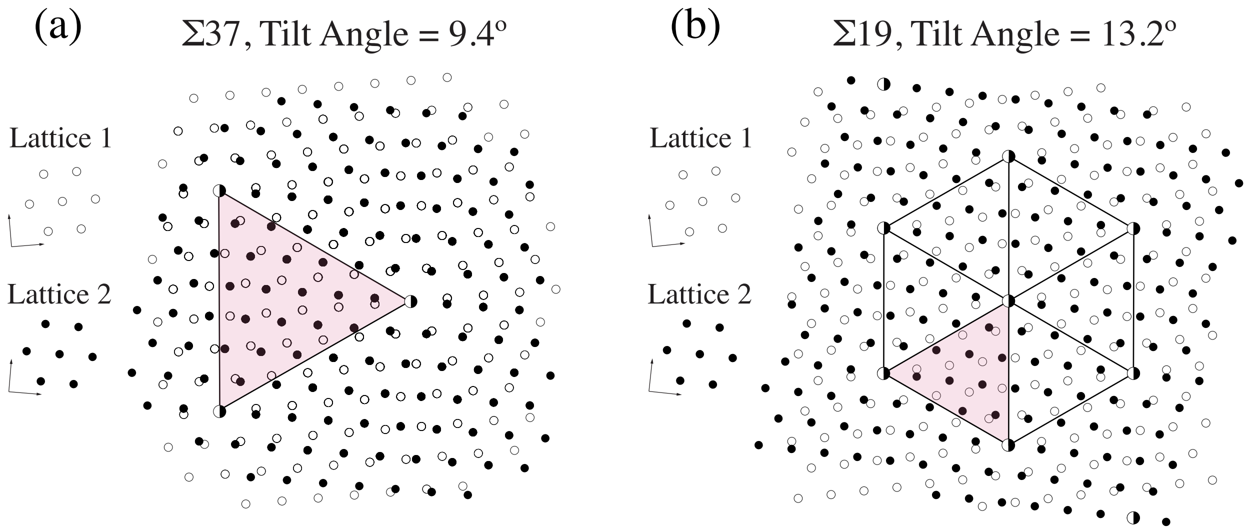

Figure S1: Dichromatic pattern of the (a) Σ37 and (b) Σ19 GBs. Empty and filled markers represent sites from lattice 1 and lattice 2, respectively, while coincident lattice sites are shown as half-filled circles. Overlaid triangles indicate regions connecting three such coincident sites.

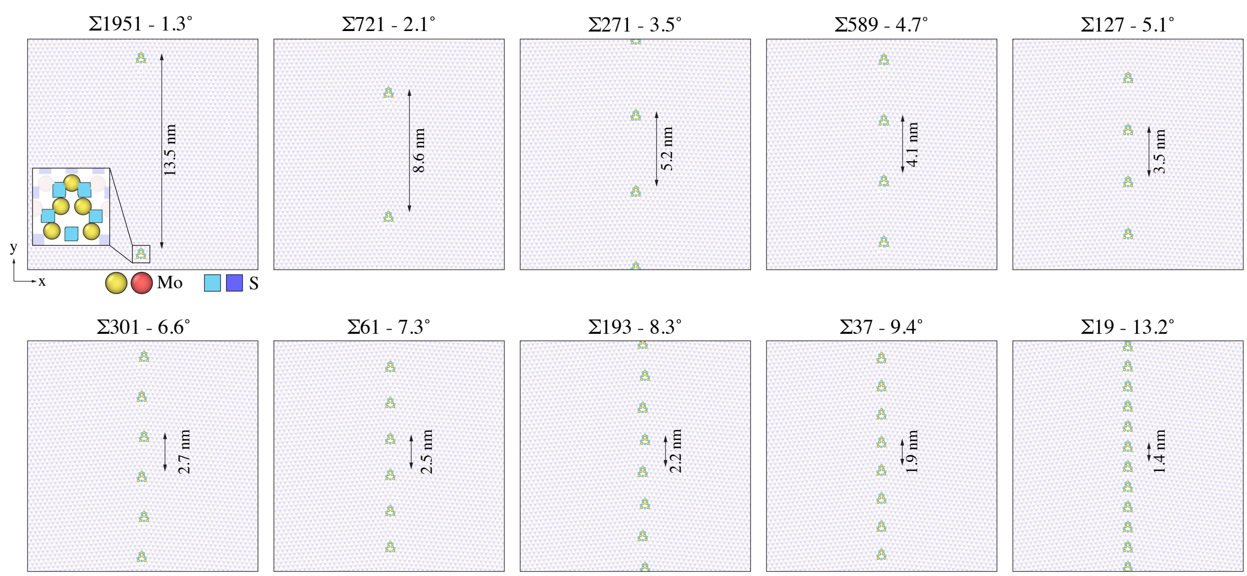

Figure S2: Atomic structures for all grain boundary misorientations examined in this work. Molybdenum (sulfur) atoms are colored gold/red (teal/blue). The boundary structures are composed of 5|7 ring motifs whose spacing decreases with increasing the misorientation angle.

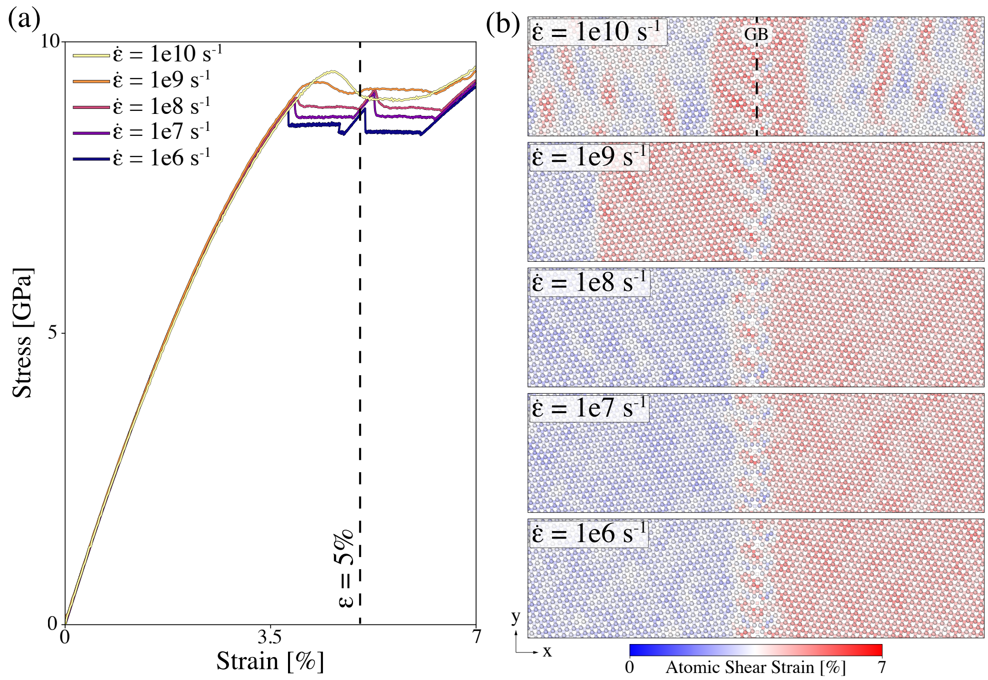

Figure S3: For the Σ19 GB with a misorientation angle of 13.2°: (a) strain-rate dependence of the tensile deformation behavior at 10 K. (b) At an applied tensile strain of 5%, snapshots depicting the atomic structures colored by the per-atom shear strain for different strain-rates.

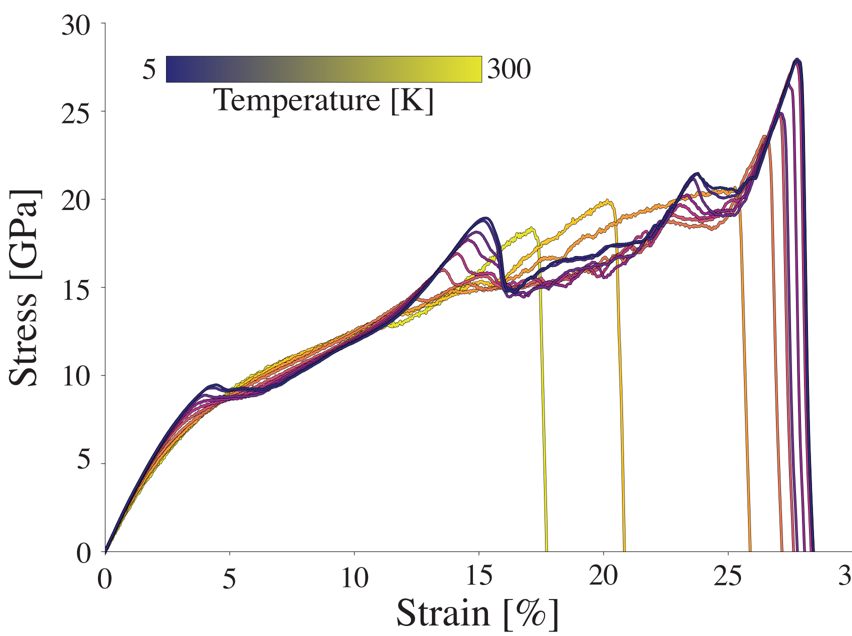

Figure S4: For the Σ19 GB with a misorientation angle of 13.2°, stress-strain curves at temperatures ranging from 5 K to 300 K. Each curve is colored by the corresponding temperature.

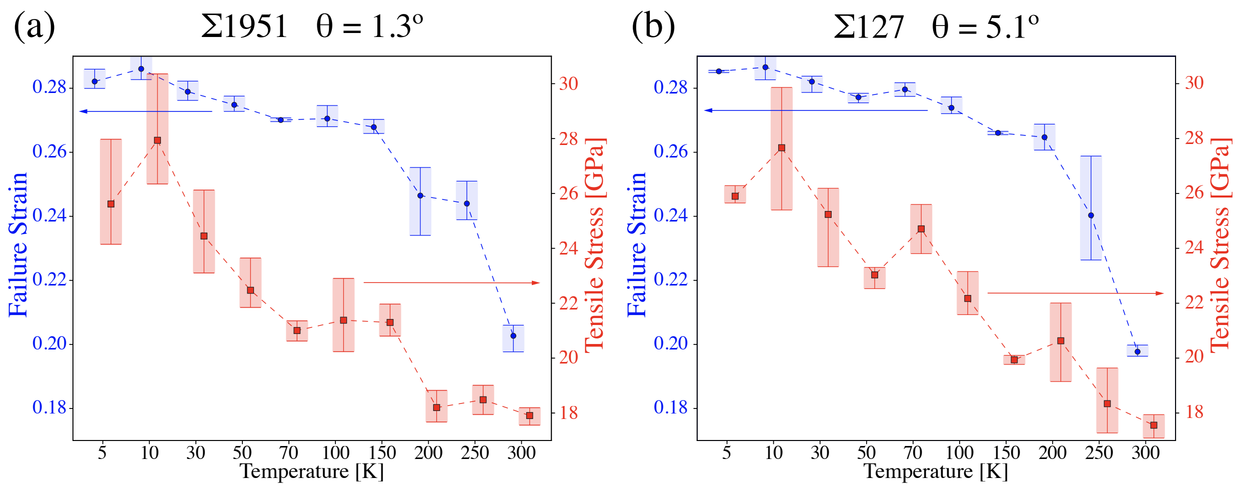

Figure S5: The ultimate tensile stress and ultimate failure strain as a function of temperature for GBs with a misorientation angle of (a) 1.3° (Σ1951) and (b) 5.1° (Σ127). Each point represents the mean of three runs with the error bars indicating the maximum and minimum values.

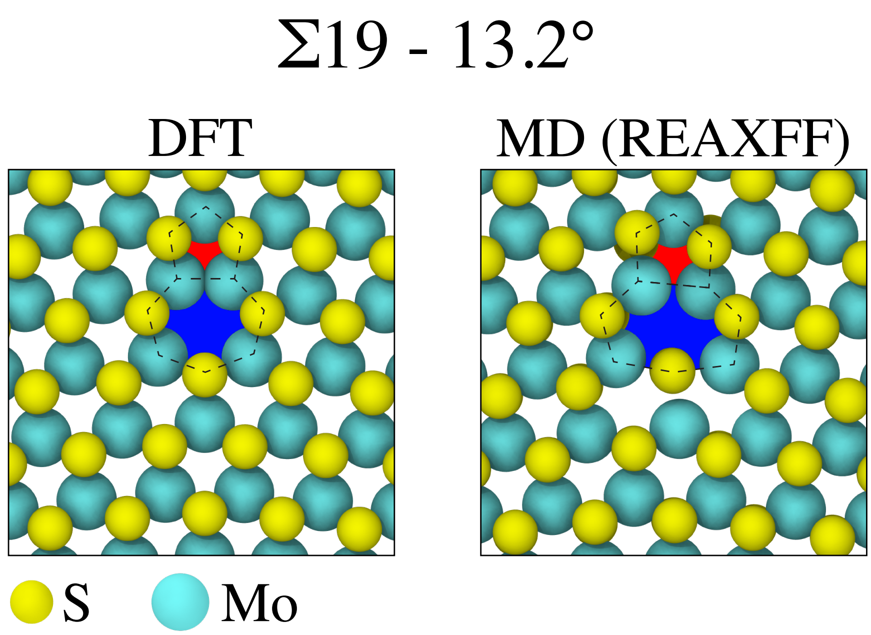

Figure S6: For the GB with a misorientation angle of 13.2°, GB structure predictions using DFT and classical atomistic simulations employing the ReaxFF used in this work.

DFT simulations were performed in VASP,[S1,S2] using the Perdew, Burke and Ernzerhof generalized gradient approximation exchange-correlation functional[S3] with empirical dispersion corrections added using the DFT-D3-BJ scheme.[S4,S5] A plane-wave cutoff of 520 eV was used with Gaussian smearing with a 0.05 eV smearing width. For the self-consistent field optimization, a convergence tolerance of 10^{-5} eV was used. Ionic relaxations were performed until all forces were less than 0.01 eV/Å. A $1 \times 8 \times 1$ Monkhorst-Pack scheme was used for k-point sampling[S6] with a "normal" flag set for integration. For a GB with a misorientation angle of 13.2°, Fig. S6 shows boundary structure predictions using DFT and the ReaxFF potential used in this work, where it can be seen that both simulation methods predict similar structures for the 5|7 ring motifs.

References

(S1) Kresse, G.; Furthmüller, J. Efficiency of ab-initio total energy calculations for metals and semiconductors using a plane-wave basis set. *Physical Review B* **1996**, *54*, 11169–11186.

(S2) Kresse, G.; Joubert, D. From ultrasoft pseudopotentials to the projector augmented-wave method. *Physical Review B* **1999**, *59*, 1758–1775.

(S3) Perdew, J. P.; Burke, K.; Ernzerhof, M. Generalized Gradient Approximation Made Simple. *Physical Review Letters* **1996**, *77*, 3865–3868.

(S4) Grimme, S.; Antony, J.; Ehrlich, S.; Krieg, H. A consistent and accurate *ab initio* parametrization of density functional dispersion correction (DFT-D) for the 94 elements H–Pu. *Journal of Chemical Physics* **2010**, *132*, 154104.

(S5) Grimme, S.; Ehrlich, S.; Goerigk, L. Effect of the damping function in dispersion corrected density functional theory. *Journal of Computational Chemistry* **2011**, *32*, 1456–1465.

(S6) Monkhorst, H. J.; Pack, J. D. Special points for Brillouin-zone integrations. *Physical Review B* **1976**, *13*, 5188–5192.